Pergamon

Int. J. Multiphase Flow Vol. 23, No. 4, pp. 699–712, 1997

Printed in Great Britain
PII: S0301-9322(97)00003-7
0301-9322/97 $17.00 + 0.00

INSTABILITY ANALYSIS OF THE TRANSITION FROM BUBBLING TO JETTING IN A GAS INJECTED INTO A LIQUID

K. CHEN and H. J. RICHTER
Thayer School of Engineering, Dartmouth College, NH 03755, U.S.A.

(Received 2 September 1996; in revised form 22 January 1997)

Abstract—Submerged gas injection into liquids is a widely applied processing technique. At low gas flow rates, a bubble plume forms in the liquid. With increasing gas flow rates, the gas bubbles in the plume coalesce and a gas jet is formed. Transition from bubbling to jetting occurs in the transonic region. To date, there is no sufficient theoretical explanation for this transition. In this paper, a basic theory is developed to explain the transition from bubbling to jetting. The instability of a circular compressible gas jet in a liquid was studied. For the axisymmetric mode, it was found that there is a peak growth rate for both the temporal and spatial instabilities when the Mach number approaches unity. The instability quickly reduces to vanishing values at supersonic gas velocities. However, in the supersonic region, it was shown that the helical instability mode may become important. Gas pressure perturbations have a destabilizing effect in the subsonic region but a stabilizing effect in the supersonic region. The problem of absolute instability was studied in order to explain the physical phenomenon of the transition from bubbling to jetting. Absolute instability was found in the subsonic region and a gas jet always breaks up into bubbles in the subsonic region. No absolute instability was found in the supersonic region, and the gas jet may remain stable. This transition from absolute to non-absolute instability occurs in the transonic region which was observed to be the transition from bubbling to jetting. © 1997 Elsevier Science Ltd.

Key Words: bubbling, jetting, instability, temporal, spatial, absolute, subsonic, supersonic

1. INTRODUCTION

The process of submerged gas injected into a liquid environment is described in figure 1. This is important in metallurgical processes, which involve high temperatures. Submerged bubbling/jetting is employed to enhance heat and mass transfer rates by producing large interfacial areas. The whole gas-stirred injection zone consists of several regions, a gas bubbling or jetting core, a two-phase turbulent zone of gas dispersed in liquid, a liquid recirculating zone, and sloshing waves formed on the surface of the bath when the gas flow rate is high enough.

With increased gas injection flow rate, a transition from *bubbling* to *jetting* occurs when the bubbles in the plume coalesce, thus a gas jet is formed. In the initial jetting regime, the gas jet does not disintegrate until it reaches some distance from the nozzle, where the jet breaks up into a column of rising bubbles. The transition between bubbling and jetting can be identified. There is a change in the sound generated by the gas flow. Jetting corresponds to a high frequency sound while bubbling is characterized by a deep, low frequency sound (Payne and Prince 1975). Also the bubbling is seen to expand radially from the injector and essentially no expansion is seen in the jetting regime (Ozawa and Mori 1983).

McNallen and King (1982) tested the injection of different inert gases into water and liquid metals and concluded a criteria for transition to jetting nozzle exit mass flux of about 40 g/cm^2 s. This value corresponds to sonic injection in an air–water system at environmental pressure. Ozawa and Mori (1983) stated that the transition from bubbling to jetting takes place when the nominal Mach number at the injection nozzle exit approaches unity. They used the ratio of the time during which the basal diameter of bubbles or jets is in apparent contact with the orifice diameter to a total observing time. There is an abrupt reduction of time fraction of contact at the transonic region. The phenomenon is similar both for gas injected into water and mercury. Ozawa and Mori did not give a theoretical explanation on the transition from bubbling to jetting. Koria (1993) presented a simple structure model and calculated the non-buoyant jet length. He concluded that

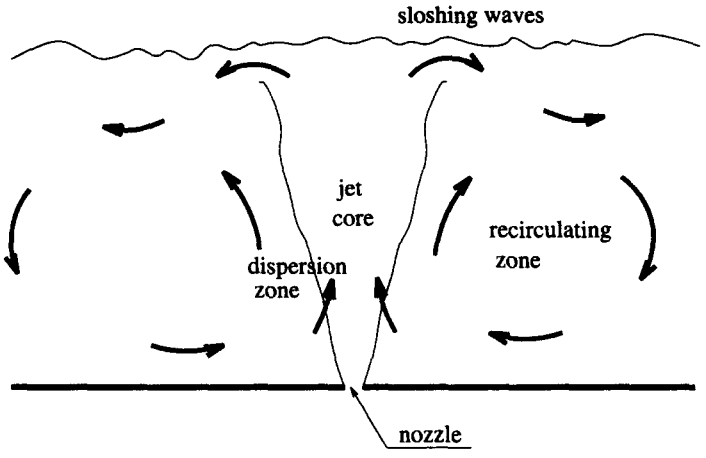

Figure 1. Submerged blowing of a gas into a liquid in metallurgical processes.

for injection velocities of $M < 1$, the gas jet disintegrates in the form of bubbles very close to the gas injecting orifice, and a bubble column forms in a metal bath. For $M > 1$, the length of the non-buoyant jet in the bath is appreciable and the jet disintegrates later into bubbles.

The transition from gas bubbling to jetting is very important because high gas injection velocity is necessary to obstruct liquid accretion formation on the tip of the injection nozzle and to prevent the phenomenon of gas back attack, but jetting may reduce the reactant interfacial contact area and gas residence time, thus reducing heat and mass transfer between the phases. However, there is little fundamental explanation presented with regard to these important phenomena. The present research is focusing on improving the current theoretical understanding of the transition from bubbling to jetting.

2. MATHEMATICAL MODEL

There are two ways to consider the mathematical model of gas bubbling or jetting into a liquid bath. As gas injection flow rates increase from small values, the bubble frequency is increasing. The bubbles form, rise, coalesce or break up to form a relatively stable bubble plume. Prince and Blanch (1990) proposed a model to calculate the rates of bubble coalescence and bubble breakup in turbulent gas–liquid dispersions. They used the Monte Carlo simulation for the experimental measurements of coalescence and breakup events. However, Prince and Blanch's calculations and experiments were at low gas flow rates, which are far from the sonic region. This model cannot be extrapolated to predict the transition from gas bubbling to jetting. Zhao and Irons (1989) gave a theoretical explanation for the transition from gas bubbling to jetting. They argued that the breakup of large bubbles cause by Raleigh–Taylor and Kelvin–Helmholtz instability will entrain liquid droplets into the gas. Finally, the gas flows continuously and jetting occurs. However, their fundamental theory can be questioned because it was based on single bubble breakup, yet it is not observed that the bubbles at the orifice first break up into many small bubbles before coalescing to form a jet.

In our approach, we consider a gas jet at sufficiently high gas flow rates. If we reduce the gas flow rate, the gas jet may break up into bubbles. Little research work has been reported for a high-velocity compressible gas jet in a liquid environment. Theoretical analysis can be resorted to give a characteristic description of the gas jet breakup. Instability theory is used here which deals with the interfacial waves without consideration of liquid entrainment. C.iang and Russel (1965) did linear subsonic and supersonic analyses respectively for a specific gas–liquid system. In their study, the sonic point was identified as a singularity (infinite growth rate), and the wave velocity of the disturbance was assumed to be negligible. Chawla (1975) included a non-zero wave velocity in his study of the stability of a sonic gas jet submerged in a liquid. However, his numerical results pertain only to a Mach number of unity. The classic temporal instability analysis has been extended

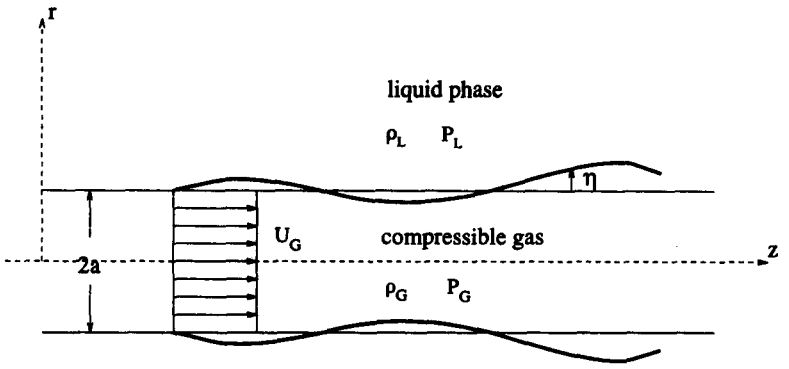

Figure 2. Sketch of the mathematical model.

to a spatial instability analysis (Leib and Goldstein 1986; Zhou and Lin 1992; Li 1992), and the concepts of convective and absolute instability were established (Sturrock 1958; Briggs 1964; Monkewitz 1990). However most of the modern instability analyses focus on liquid-jet instability in a gas environment. Little research deals with gas jet instability in a liquid environment which is the topic of this paper.

A simplified model is given here to investigate the stability of an isentropic, compressible gas jet injected from a circular cylindrical nozzle with radius a, into an unbound inviscid liquid environment. The gas jet is considered to be homogeneous, of uniform velocity profile, semi-infinite system. Gravity is negligible if the gas velocity is high and the gas inertia is dominant (figure 2).

The conservation equations of mass and momentum for the gas and the liquid phase are

$$\frac{\partial \rho_i}{\partial t} + \nabla\cdot(\rho_i \mathbf{V}_i) = 0, \tag{1}$$

$$\rho_i\left(\frac{\partial}{\partial t} + \mathbf{V}_i\cdot\nabla\right)\mathbf{V}_i = -\nabla P_i, \tag{2}$$

where ρ is the density, $\mathbf{V}_i$ is the velocity vector, P is the dynamic pressure and index i = G, L denotes the gas or liquid phase. Taking the perturbations of the above equations, canceling the basic state and retaining only the linear terms, we have

$$\left(\frac{\partial}{\partial t} + \delta_{Gi}U_G\frac{\partial}{\partial z}\right)\mathbf{V}_i' = -\frac{1}{\bar{\rho}_i}\nabla P_i'. \tag{3}$$

$$\left(\frac{\partial}{\partial t} + \delta_{Gi}U_G\frac{\partial}{\partial z}\right)\rho_i' = -\bar{\rho}_i\nabla\cdot\mathbf{V}_i', \tag{4}$$

where primes are used to designate the perturbations of the variables, U_G is the gas mean velocity and δ_{Gi} is 1 or 0 depending upon if i = G or i = L.

The linearized kinematic and dynamic boundary conditions are

$$V_{ir}' = \frac{\partial \eta}{\partial t} + \delta_{Gi}U_G\frac{\partial \eta}{\partial z}, \tag{5}$$

$$P_G' - P_L' = S\left(\frac{\eta}{a^2} - \frac{1}{a^2}\frac{\partial^2\eta}{\partial\theta^2} - \frac{\partial^2\eta}{\partial z^2}\right) \tag{6}$$

at $r = a + \eta$, where η is the interface displacement, r is the radial distance, V_{ir} is the velocity component in the radial direction, θ is the azimuthal angle and z is the downstream distance from the nozzle. S is the surface tension and $\mathbf{n}$ is the direction normal to the interface. P_L', $\mathbf{V}_L'$ are limited

values when $r \to \infty$. Taking the divergence of [3] and then using [4], the following equation is achieved

$$\left(\frac{\partial}{\partial t} + U_G \frac{\partial}{\partial z}\right)^2 \rho_i' = \nabla^2 P_i'. \qquad [7]$$

Assuming the change of gas pressure with respect to density is an isentropic process, we have

$$P_G' = \left.\frac{\partial P_G}{\partial \rho_G}\right|_s \rho_G' = c_G^2 \rho_G', \qquad [8]$$

where s is the entropy and c_G is the sound velocity. Substituting [8] into [7], we get for the gas phase,

$$\left(\frac{\partial}{\partial t} + U_G \frac{\partial}{\partial z}\right)^2 P_G' = c_G^2 \nabla^2 P_G'; \qquad [9]$$

while for the liquid phase

$$\frac{\partial^2 P_L'}{\partial t^2} = 0. \qquad [10]$$

If both sides of [5] are taken by $(\partial/\partial t) + \delta_{Gi} U_G (\partial/\partial z)$, using [7], the kinematic condition will become

$$\left(\frac{\partial}{\partial t} + \delta_{Gi} U_G\right)^2 \eta = -\frac{1}{\bar{\rho}_i} \frac{\partial P_i'}{\partial r}. \qquad [11]$$

The standard method of normal modes is used to satisfy the linearized equations. Let

$$\begin{Bmatrix} P_L' \\ P_G' \\ \eta \end{Bmatrix} = \begin{Bmatrix} \bar{\rho}_L U_G^2 p_L(r) \\ \bar{\rho}_L U_G^2 p_G(r) \\ a\xi \end{Bmatrix} \exp[i(KZ + n\theta - \Omega\tau)]. \qquad [12]$$

p_G and p_L are the respective dimensionless pressures. K and Ω are dimensionless wave number and angular frequency respectively and the integer n specifies the periodicity of the motion around the cylinder circumference. (R, Z, ξ) and τ are defined as

$$(R, z, \xi) = (r, z, \eta)/a,$$

$$\tau = \frac{t U_G}{a}. \qquad [13]$$

Substituting [12] into [9] and [10] leads to the governing equations for the dimensionless perturbation pressure amplitudes

$$\{D^2 + R^{-1}D - [n^2 R^{-2} + K^2 - M^2(K - \Omega)^2]\} p_G = 0, \qquad [14]$$

$$\{D^2 + R^{-1}D - [n^2 R^{-2} + K^2]\} p_L = 0, \qquad [15]$$

in which $D = \mathrm{d}/\mathrm{d}z$ and $M = U_G/c_G$. The corresponding boundary conditions at $R = 1$ are

$$p_L - p_G + \mathrm{We}(K^2 + n^2 - 1)\xi = 0,$$

$$\Omega^2 \xi - \frac{\partial p_L}{\partial R} = 0,$$

$$Q(K - \Omega)^2 \xi - \frac{\partial p_G}{\partial R} = 0, \qquad [16]$$

where the dimensionless numbers are defined as

$$\mathrm{We} = \frac{S}{\bar{\rho}_L U_G^2 a}, \quad Q = \frac{\bar{\rho}_G}{\bar{\rho}_L}. \tag{17}$$

The bounded solutions for [14] and [15] are

$$p_L = AK_n(KR),$$
$$p_G BI_n(\lambda R). \tag{18}$$

$K_n()$, $I_n()$ are modified Bessel functions and $\lambda$is defined as

$$\lambda = \sqrt{K^2 - M^2(K-\Omega)^2}. \tag{19}$$

Substituting [19] into [16] yields

$$A = \frac{\Omega^2 \xi}{KK_n'(K)},$$
$$B = Q\frac{(K-\Omega)^2\xi}{\lambda I_n'(\lambda)}. \tag{20}$$

Finally, the dispersion equation is

$$\frac{\Omega^2 K_n(K)}{KK_n'(K)} - \frac{Q(K-\Omega)^2}{\lambda I_n'(\lambda)} I_n(\lambda) - \mathrm{We}(1 - K^2 - n^2) = 0, \tag{21}$$

where primes denote the differentiation $\partial/\partial(\lambda R)$. For a given set of flow parameters We, Q and M, this governing dispersion equation gives the relationship of the dimensionless wave frequency Ω and the dimensionless wave number K. The dispersion equation will lead to Rayleigh's equation for a hollow jet in a liquid (Rayleigh 1879), if the density ratio equals zero and the axisymmetric mode is used. Moreover, in the limiting case that K approaches infinity, the dispersion equation [21] is reduced to the characteristic equation obtained by Taylor (1945) if viscous terms are omitted.

3. NUMERICAL RESULTS AND ANALYSIS

The dimensional perturbation expression in [12] is $\exp[i(kz + n\theta - \omega t)]$. The two cases of most interest are those in which either k or ω is real. A wave is said to be temporal unstable if for some real wave number k, a complex $\omega = \omega_r + i\omega_i$ is obtained with positive ω_i, which denotes growth in time of a spatially periodic disturbance of infinite extent. ω_i is called temporal growth rate. Oppositely, if k is allowed to be a complex number for a real frequency ω, i.e. $k = k_r + k_i$, it is called spatial instability which describes the downstream evolution of a constant-amplitude harmonic input at some starting position, and $-k_i$ is called spatial growth rate. Gaster (1962) demonstrated theoretically the relation between temporal growth rate and spatial growth rate by integrating the Cauchy–Riemann relation.

The axisymmetric mode ($n = 0$) is studied primarily in this research. The calculation results of limited cases of non-axisymmetric modes will be presented to compare with the axisymmetic mode. The classical Newton's method was used throughout the numerical calculation of the dispersion equation.

Figure 3 shows the dimensionless temporal growth rate Ω_i against the dimensionless wave number K for two different gas to liquid density ratios Q. The flow is in the subsonic region ($M = 0.5$). The temporal growth rate increases with increasing wave number. Increasing the density of the surrounding liquid has a stabilizing effect by decreasing the growth rate in the subsonic region. The figure only includes a limited range of wave numbers. The nearly linear curve of the temporal growth rate with an increase in wave number will level out and decrease when the wave number increases further. Figure 4 shows two cases of temporal growth rate for different Weber numbers in the subsonic region. Increasing the Weber number will decrease the growth rate in the large wave number regions and this effect becomes more obvious as the wave number

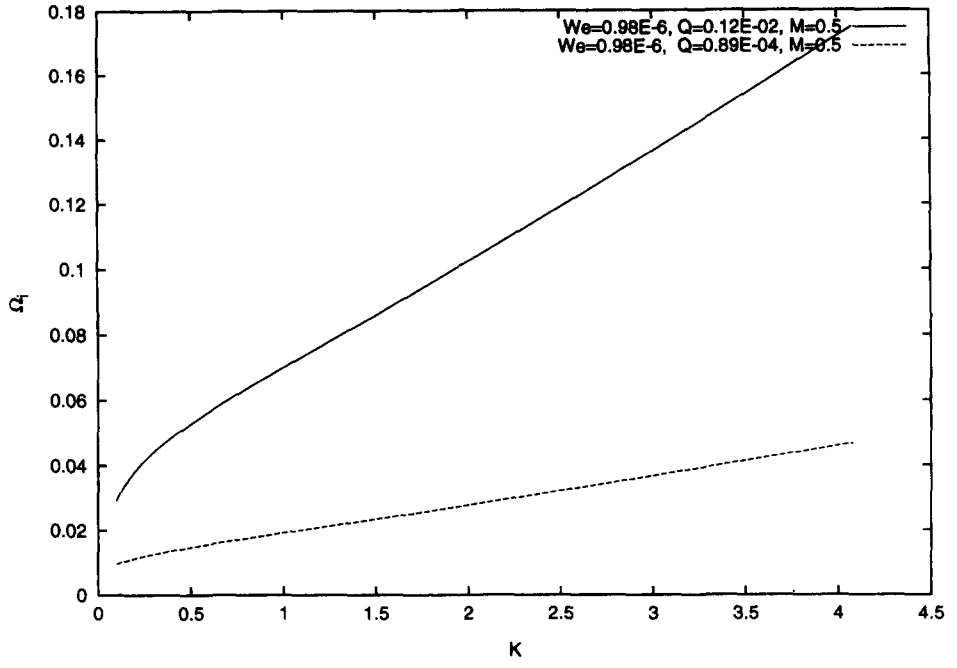

Figure 3. Temporal growth rate versus wave number with different density ratios.

increases, which means surface tension has a stabilizing effect on the waves with short wave lengths in the subsonic region.

The temporal growth rate versus the Mach number is shown in figures 5–7 for different density ratios, surface tensions and wave numbers. The temporal growth rate increases first as the Mach number increases in the subsonic region, reaches the maximum point where the Mach number approaches unity, and quickly reduces to vanishing values after that. The first two curves give the temporal growth rates for the density and the surface tension corresponding to the air–water system

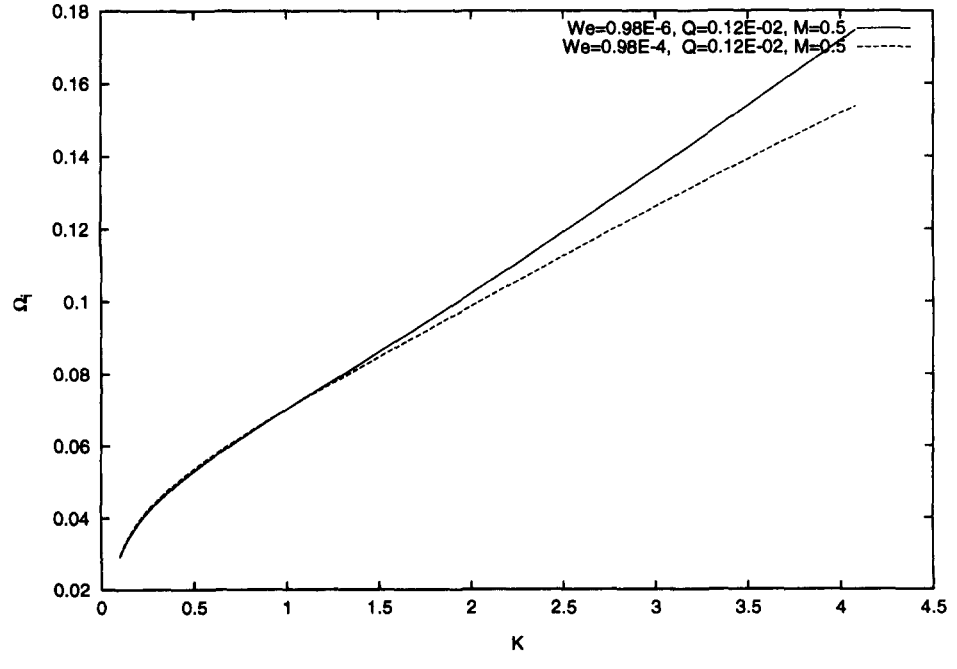

Figure 4. Temporal growth rate versus wave number with different Weber numbers.

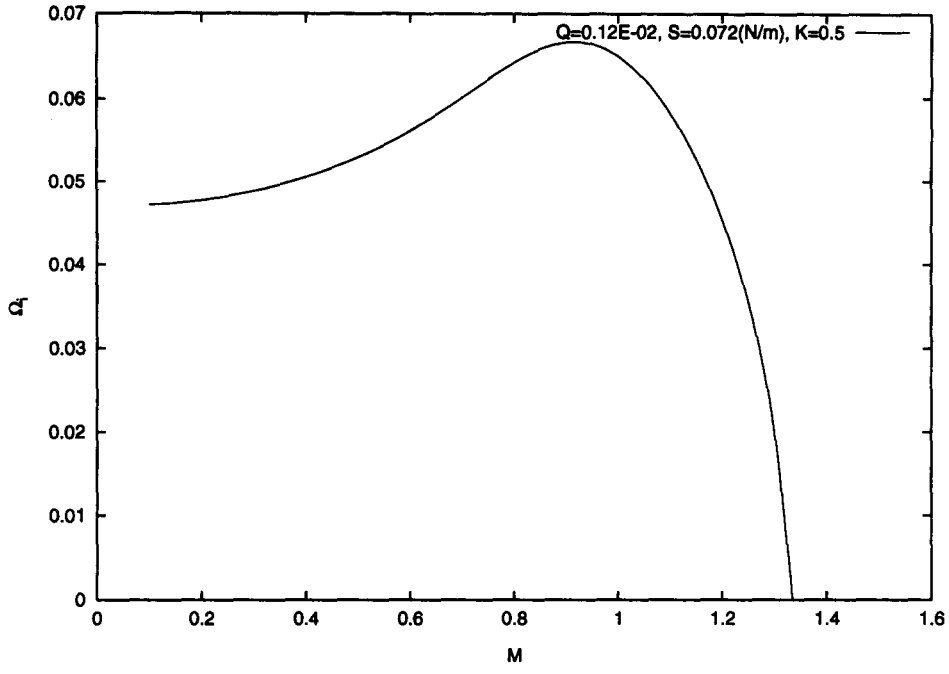

Figure 5. Temporal growth rate versus Mach number: air–water system, $K = 0.5$.

and air–mercury system, while a different dimensionless wave number $K = 2\pi$ was used in the third curve for air–mercury. At the transonic region, a similar peak of temporal growth rate was obtained for all three cases. The theoretical study shows that the gas jet undergoes the most unstable situation when the Mach number approaches unity and the gas jet becomes temporally stable in the supersonic region.

Figures 8 and 9 show the spatial growth rates of two cases, corresponding to the air–water and the air–mercury system. The tendency of the spatial growth rate approaching zero at the supersonic

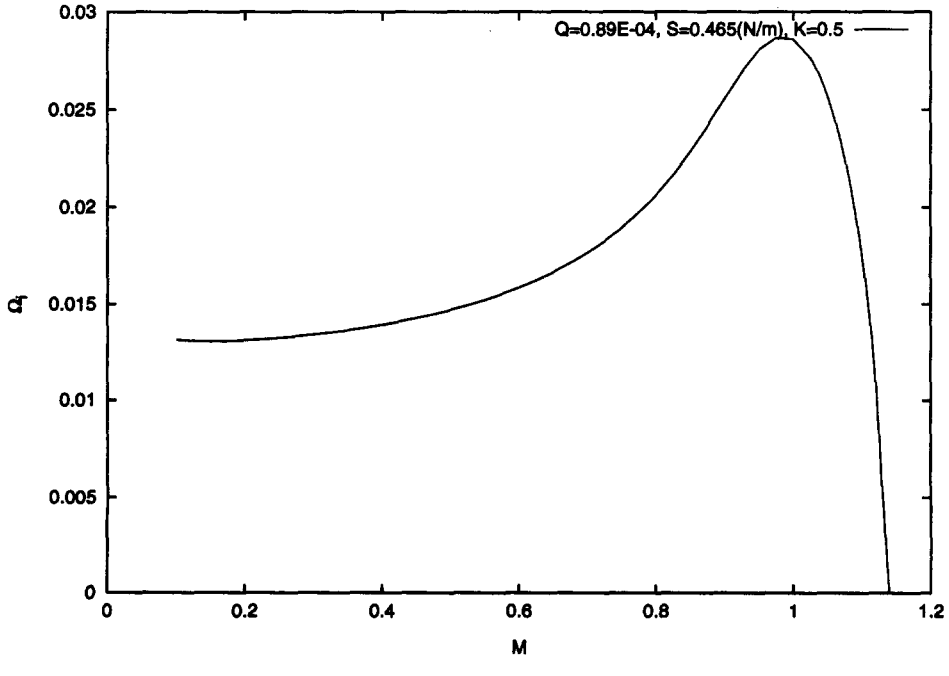

Figure 6. Temporal growth rate versus Mach number: air–mercury system, $K = 0.5$.

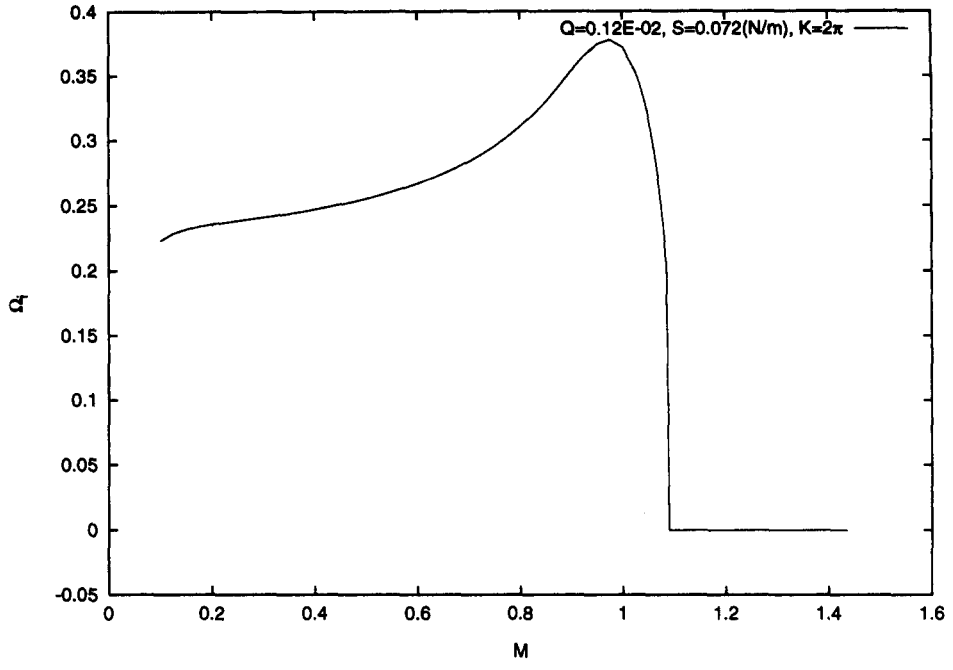

Figure 7. Temporal growth rate versus Mach number: air–water system, $K = 2\pi$.

region is the same as that of the temporal cases. The spatial growth rate undergoes a maximum value in the sonic region, then dramatically reduces to a vanishing value when the supersonic region is reached. A gas jet is always spatially unstable in the subsonic region and becomes stable in the supersonic region. If we write the downstream coordinate z as $z = Vt + z_0$, it can be shown that an observer moving with velocity $V_0 = \partial\omega_r/\alpha k_r|_{k_r = k_0}$, will see the disturbance increase as $\exp(\sigma_0 t)$, where σ_0 is the maximum positive imaginary part of ω for real k (Briggs 1964). $\partial\omega_r/\partial k_r$ is also called group velocity. It was calculated that the group velocity of the air–water system is much smaller

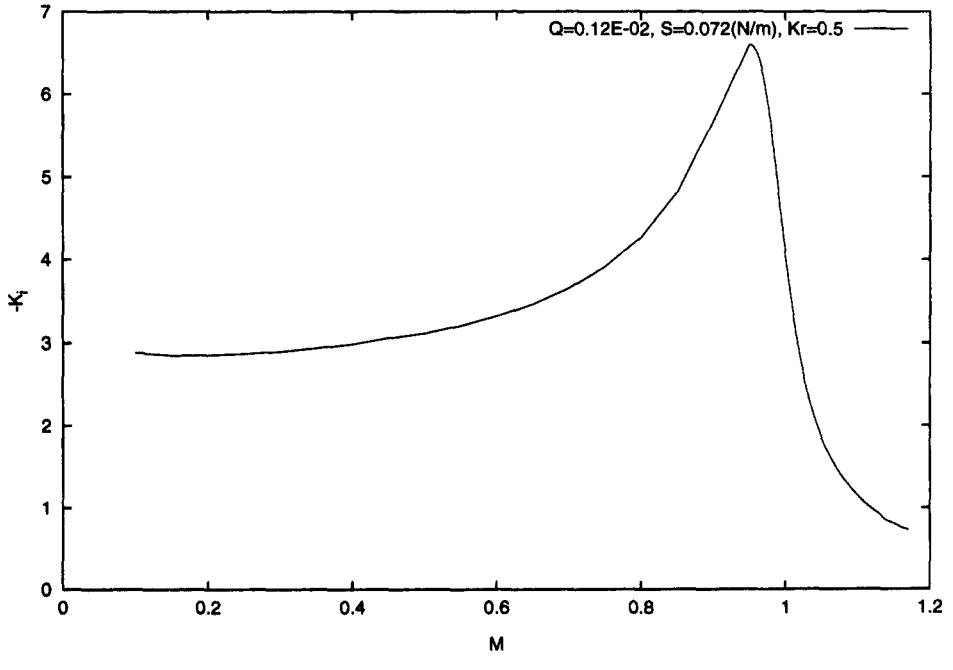

Figure 8. Spatial growth rate versus Mach number: air–water system.

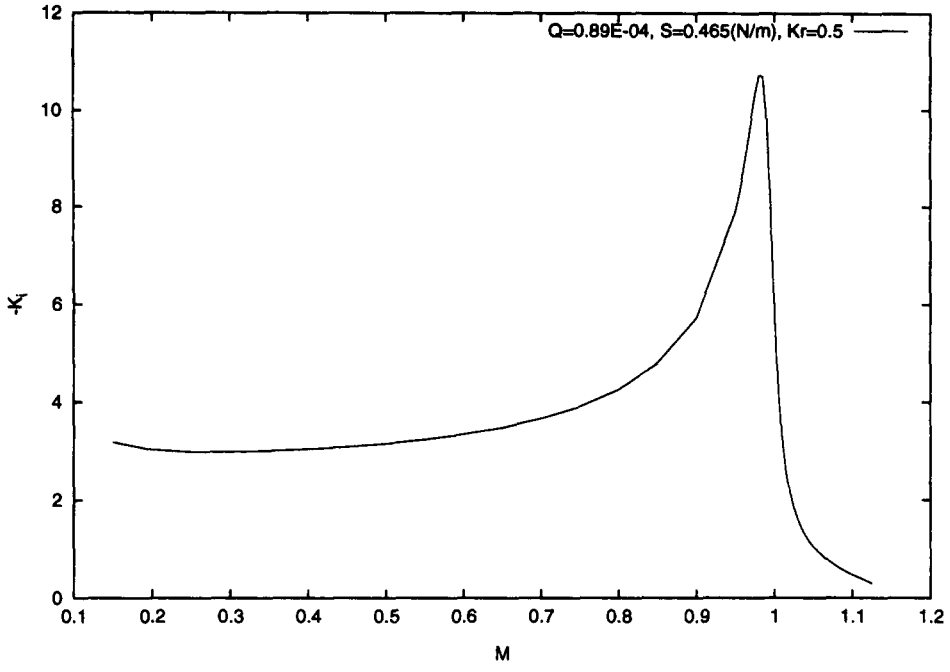

Figure 9. Spatial growth rate versus Mach number: air–mercury system.

than that of the air–mercury system under the same conditions. Because the group velocity denotes the propagation velocity of the disturbances, the effect of faster propagation velocity offsets the effect of faster disturbance growth of the air–water system, and the differences of spatially growing disturbances between air–water and air–mercury systems become much smaller. The importance of liquid density on group velocity is physically obvious, since the interface wave needs to overcome liquid inertia for propagation.

Only results for the axisymmetric mode ($n = 0$) have been presented so far. It is argued that the non-axisymmetric modes may become important when the velocity differences through the interface become large. The effects of the first non-axisymmetric mode (helical mode, $n = 1$) have been recorded in experiments with high-speed liquid jets moving in the air (Hogt and Taylor 1977). Here we give the results of the temporal instability for the helical mode and the second non-axisymmetric mode ($n = 2$). Figure 10 shows the comparison of the temporal growth rates of the axisymmetric mode and the helical mode respectively, for $K = 1$. For low jet velocity, the axisymmetric mode dominates. As the jet velocity increases, the temporal growth rate of the axisymmetric mode decreases rapidly in the transonic region, while the temporal growth rate of the helical mode keeps increasing until the Mach number reaches about 2.0. That is, the temporal growth rate of the helical mode has a peak growth rate occurring at a Mach number much larger than the axisymmetric mode. Thus, the axisymmetric mode is dominated by the helical mode in the supersonic region. This is understandable if the velocity component of the supersonic flow in the helical wave direction is still subsonic while it reaches supersonic region for the axisymmetric mode. Figure 11 gives the comparison of the temporal growth rates of a higher non-axisymmetric mode of $n = 2$ and the axisymmetric mode. The temporal growth rate of $n = 2$ mode experiences a sudden change in the sonic region and goes to vanishing values in the supersonic region, and is less than that of the axisymmetric mode in the subsonic region.

The fundamentals of the interfacial instability caused by pressure perturbation, namely Kelvin–Helmholtz instability can be conveniently explained by the concept of a vortex sheet, and its instability (Batchelor 1967). The compressibility evidently has an important effect on flow instability. Li (1992) gave a brief explanation of the effect of the compressibility based on the cortex theory. He argued that in the subsonic region, the flow field around accumulated points will have

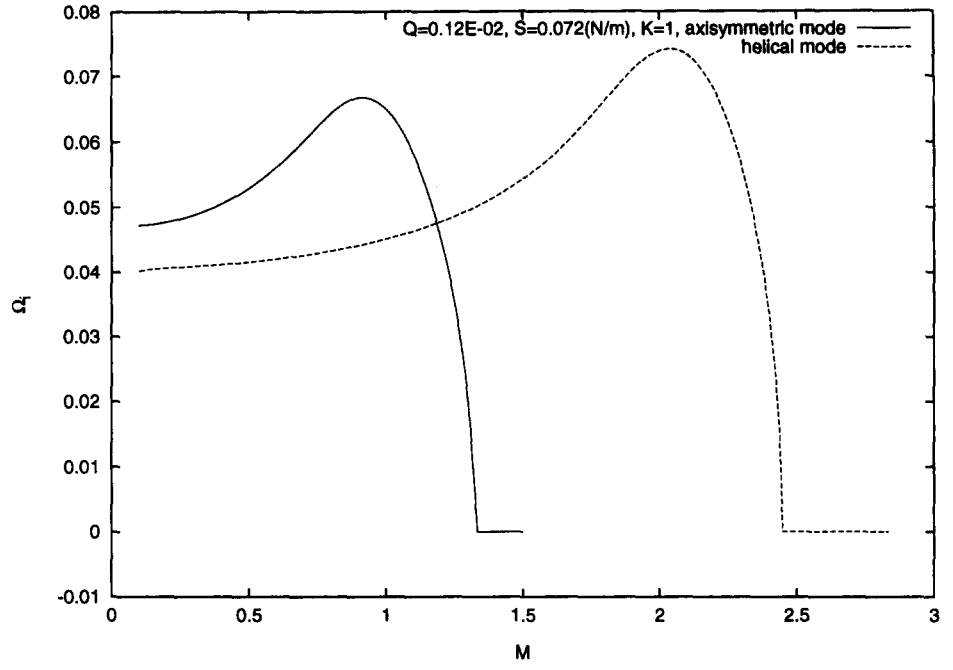

Figure 10. Comparison of the axisymmetric mode and the helical mode (air–water system): temporal growth rate versus Mach number, $K = 1$.

density changes leading to acceleration of the process of vorticity accumulation. In the supersonic regime, density changes are opposite and consequently slow down the accumulation process. Thus, the gas–liquid interface will obtained the most unstable state in the sonic region.

The kinetic energy of the gas jet can be calculated to give a further understanding of the effects of gas compressibility on the instability of a gas jet in a liquid. The time rate change of the kinetic

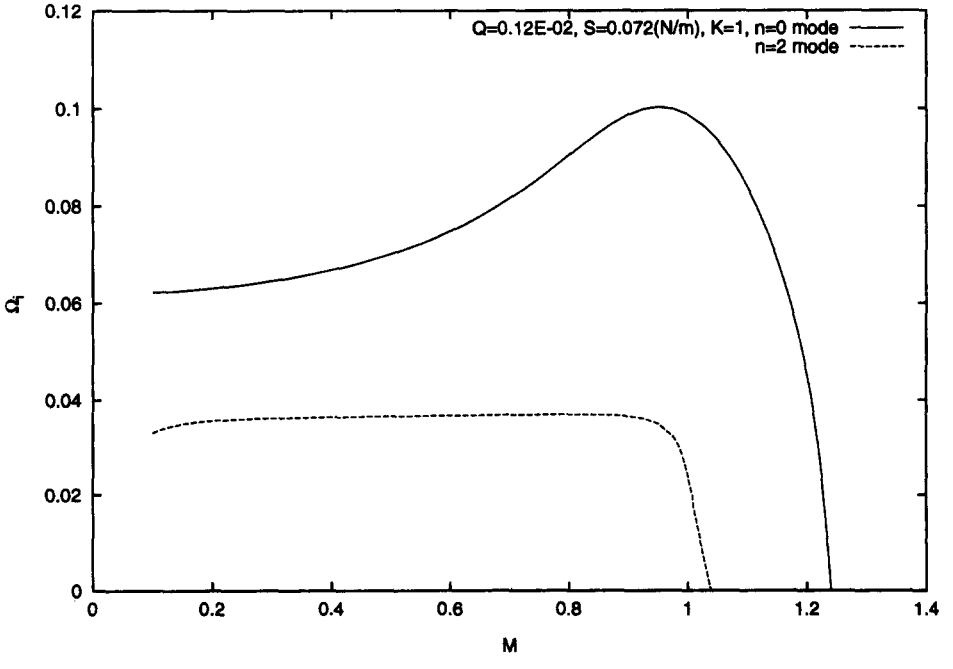

Figure 11. Comparison of the axisymmetric mode and the second non-axisymmetric mode (air–water system): temporal growth rate versus Mach number, $K = 1$.

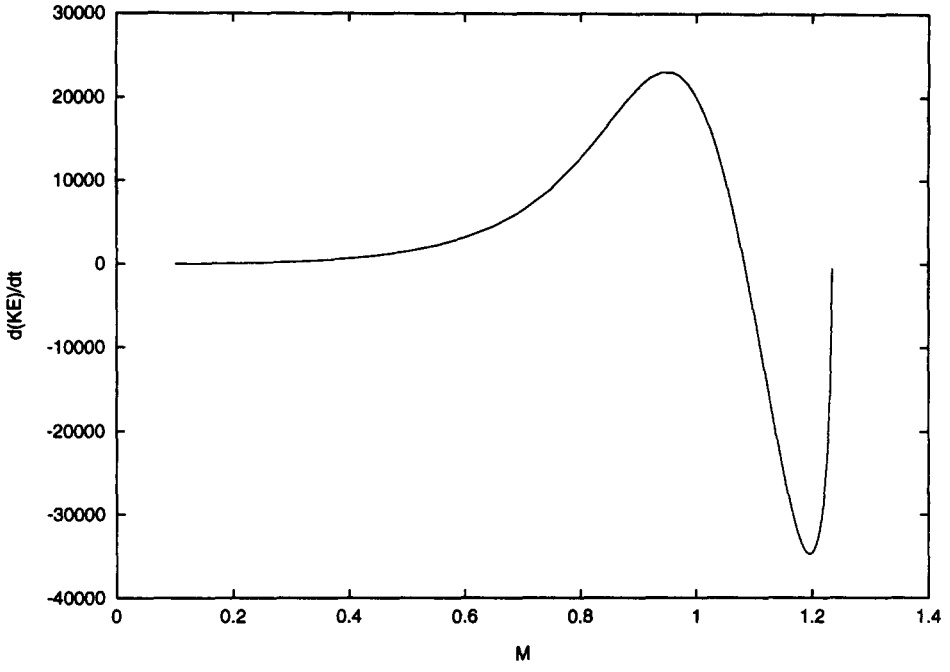

Figure 12. Time rate of kinetic energy change versus Mach number (air–water system).

energy of a gas jet is equivalent to the work done by pressure fluctuations. Thus,

$$\frac{\mathrm{d}(KE)}{\mathrm{d}t} = -\frac{1}{L}\int_0^L P'_{\mathrm{G}} u' \,\mathrm{d}z, \qquad [22]$$

where u' is the component of V'_{G} in the direction of z and L is the wavelength. Substituting the previous analysis results into [22] will eventually result in

$$\frac{\mathrm{d}(KE)}{\mathrm{d}t} = -\frac{1}{2a^2}\bar{\rho}_{\mathrm{L}} U_{\mathrm{G}}^3 \eta_0^2 \Omega_i \,\mathrm{e}^{2\Omega_i \tau}\left\{Q\frac{I_0(\lambda)(K-\Omega)^2}{\lambda(I_n)'(\lambda)}\right\}. \qquad [23]$$

The results of the calculations are shown in figure 12. The time rate change of kinetic energy increases as the Mach number increases in the subsonic region, indicating the growing instability, and reaches a maximum value near the sonic point where the jet is most unstable. Then the time rate change of kinetic energy quickly decreases in the sonic region and becomes negative at some point slightly larger than a Mach number of unity. The kinetic energy keeps changing until at some point in the supersonic region there is no change of kinetic energy. The work done by the gas pressure perturbation thus has a destabilizing effect in the subsonic region and has a stabilizing effect in the supersonic region.

In order to study the essential behavior of a system evolving and further to give a fundamental explanation of the phenomenon of transition from bubbling to jetting through the instability theory, the absolute instability should be studied. A pulse disturbance that is initially of finite spatial extent may grow in time without limit at every point in space (an absolute instability) or it may propagate along the system so that its amplitude eventually decreases with time at any fixed point in space (a convective instability) (Briggs 1964). The temporal instabilities found in the subsonic region does not mean that the jet will break up immediately at every point. The disturbances may be convected away downstream, thus the jet may break up some distance from the nozzle, which means jetting may still exist. A common criterion (Monkewitz 1990) to distinguish between absolute instability and convective instability is that absolute instability occurs at a saddle point. This corresponds to a double root of k from the dispersion equation on the complex mapping plane if $\omega_{\mathrm{o,i}} > 0$. If $\omega_{\mathrm{o,i}} < 0$, then convective instability occurs where o denotes the saddle point. To apply the criterion, the dispersion equation has to be solved for the entire range

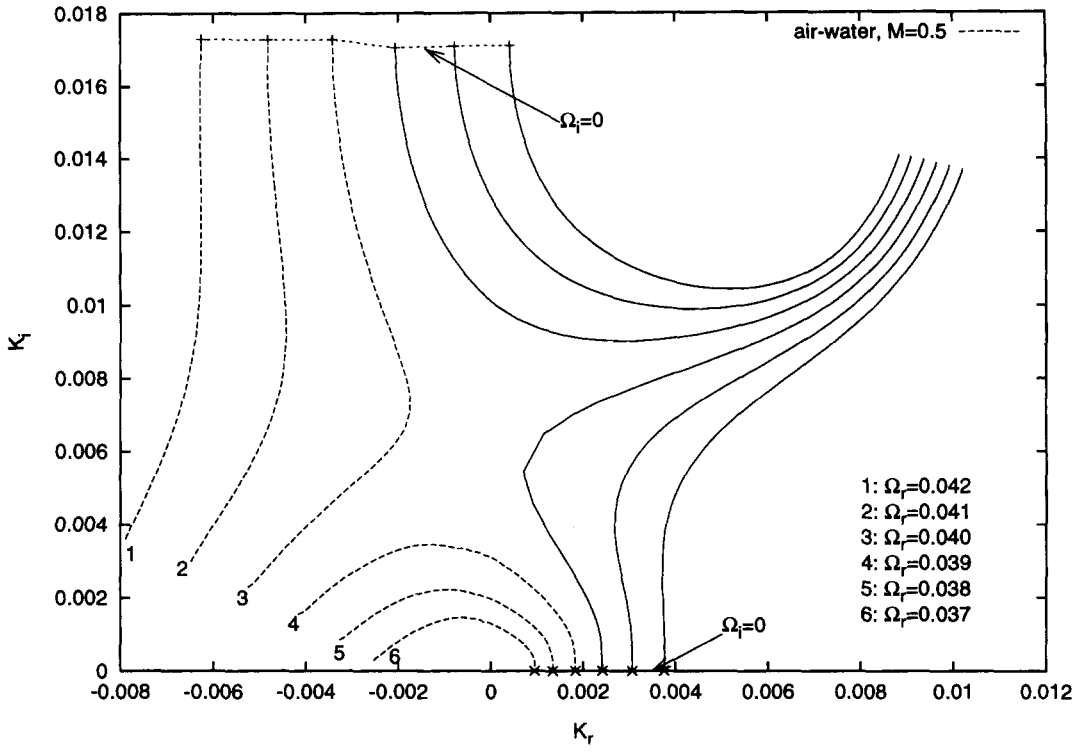

Figure 13. One pair of root loci indicating absolute instability in the subsonic region (air–water system, $M = 0.5$).

of real frequencies with varying ω_i, i.e. the mapping operation must be done for the whole complex plane.

The calculations were first done in the subsonic region. Giving various real parts of Ω, the root locus was traced in the K-plane as the positive imaginary parts of Ω were varied. Several root pairs were found. The most important root pair shown in figure 13 is the one closest to the real K axis. The loci of the roots coming from the lower half-plane represent the downstream response of an impulse source, and those coming from the upper-half plane correspond to the upstream response of the impulse source. The loci from the lower half-place cross the real axis indicating an *amplifying* wave for the loci labeled 1, 2, 3 corresponding to $\Omega_r \geqslant 0.04$. However, for the loci labeled 4, 5, 6 corresponding to $\Omega_r \leqslant 0.039$, the wave *evanescent* because the loci cross over into the upper half-plane and turn around to end up back on the real axis when $\Omega_i = 0$. The dimensionless group velocity $d\Omega/dk$ is negative for the resulting evanescent wave even though it represents a downstream propagating wave. This breakdown of the concept of group velocity was discussed by Briggs (1964). The two loci of the roots pinch at some point $\Omega_i > 0$ to form a saddle point signifying the nature of the absolute instability. The other root pairs do not cross the real axis when imaginary parts of Ω go from a positive value to zero, and no saddle points were found in these root pairs. However, the coupling roots in these root pairs first separate further as the Mach number approaches unity after the sonic region is reached. They converge together quickly at the real axis to form double roots. This behavior was referred to as a 'direct resonance' by Akylas and Benny (1980) who showed that it can increase the importance of the nonlinear effects.

The saddle point becomes deformed when the Mach number approaches unity, and no saddle points were formed in the supersonic region. Thus, the transition from absolute instability to non-absolute instability is observed numerically to fall within the transonic region. This change in local instability, that an initial disturbance will grow both temporally and spatially in the subsonic region and will become neutral or stable in fixed positions in the supersonic region, might help to explain the observed phenomenon of the transition from bubbling to jetting occurring at the transonic region. It is interesting to note that this transition from absolute instability to non-absolute instability is opposite to a liquid jet in a gas environment, where the transition was

found from convective instability in the subsonic region to absolute instability in the supersonic region (Li 1992).

4. DISCUSSION

Only the axisymmetric mode was studied in the above absolute instability analysis. Since no saddle point was found in the supersonic region and also there is no root loci across the real axis in the supersonic region, stable waves are assumed in the supersonic region which is also consistent with the previous calculations of temporal and spatial instabilities. The convective instabilities were excluded in the supersonic region. As it was first pointed out by Sturrock (1958), there is a very close connection between the concepts of amplifying waves and convective instabilities. However, as described earlier, some non-axisymmetric modes may become dominant in the supersonic region and the gas jet may not reach the stable state. The physical phenomenon of droplet entrainment and final gas jet breakup at some downstream distance indicate that amplifying waves may actually exist in the supersonic region. It is important to check in the supersonic region, whether amplifying waves (convective instabilities) exist for non-axisymmetric modes. It has been pointed out previously that in the sonic region, non-linear effects become important, thus non-linear analysis would be necessary to give more details of fluid behavior in the sonic region. Chawla established a criteria for the effectiveness of linearization as the wave velocity is not negligible compared to the gas velocity. Li (1992) gave the mathematical condition for the validation of the linearization by comparing the size of neglected nonlinear terms to that of the leading linear term.

We have not included the viscous effect of the surrounding liquid. This viscous boundary layer may become unstable and generate shear waves. The shear waves could participate with the pressure fluctuation and capillary force to bring about instabilities. This effect becomes pronounced when the wave number becomes so large that the wave length is comparable to the shear layer thickness. Li (1992) gave a simple evaluation of the shear layer effects based on the consideration of a simpler linear velocity profile with uniform density

$$\begin{aligned} u &= 1, \quad y\delta \\ u &= y/\delta, \quad \delta > y > -\delta \\ u &= -1, \quad y\delta, \end{aligned} \tag{24}$$

where δ is the thickness of the shear layer. For short waves that $k\delta > O(S/\rho_G\delta) \gg 1$, shear layer effects is important. For $O(S/\rho_G\delta) > k\delta \gg 1$, surface tension is dominant. Assuming a shear layer has the thickness δ in the order of 10^{-3}, the reliable range for this inviscid model is approximately $k < 10^4$. If the gas radius has the order of 10^{-2} then $K < 10^2$. Our calculations fit in this range.

5. CONCLUSION

The phenomenon of the transition from bubbling to jetting in gas injection through a submerged nozzle into a liquid has been studied in view of the instability of a gas jet in a liquid. A simple model of uniform-velocity profile, a semi-infinite, axisymmetric gas jet in an inviscid liquid was established and the dispersion equation was solved numerically. For the axisymmetric mode, both temporal and spatial growth rates of the disturbances increase with increasing gas velocity in the subsonic region. There is a peak of the growth rate where the Mach number approaches unity, and the growth rate quickly reduces to zero after that, which indicates interfacial waves reach the most unstable state in the sonic region and become temporally and spatially stable in the supersonic region. For long waves, the first non-axisymmetric mode becomes dominant in the supersonic region and the gas jet may not become temporally stable in the supersonic region. Absolute instability was found in the subsonic region while there is no absolute instability in the supersonic region. Thus, in the subsonic region, small disturbances will grow immediately in any position without limitation causing the jet to break up and bubbling occurs. In the supersonic region, small disturbances will finally become evanescent or be convected away

downstream so that their amplitudes eventually decrease with time, and the gas jet remains stable. Thus, jetting exists in the supersonic region and the transition from bubbling to jetting occurs in the transonic region.

REFERENCES

Akylas, T. R. and Benney, D. J. (1980) Direct resonance in nonlinear wave systems. *Studies in Appl. Math.* **63,** 209.

Batchelor, G. K. (1967) *An Introduction to Fluid Mechanics*. Cambridge University Press, Cambridge.

Briggs, R. J. (1964) *Electron–Stream Interaction with Plasmas*, Research Monograph No. 29. M.I.T. Press, Cambridge, MA.

Change, I.-D. and Russel, P. E. (1964) Stability of a liquid layer adjacent to a high-speed gas stream. *Phys. Fluids* **8,** 1018.

Chawla, T. C. (1975) The Kelvin–Helmholtz instability of the gas–liquid interface of a sonic gas jet submerged in a liquid. *J. Fluid Mech.* **67,** 513.

Gaster, M. (1962) A note on the relation between temporally-increasing and spatially-increasing disturbances in hydrodynamic stability. *J. Fluid Mech.* **14,** 222.

Hogt, J. W. and Taylor, J. J. (1977) Waves on water jets. *J. Fluid Mech.* **83,** 119.

Koria, S. C. (1993) Principles and applications of gas injection in steelmaking practice. *Scandinavian J. Metall.* **22,** 271.

Leib, S. J. and Goldstein, M. E. (1986) Convective and absolute instability of a viscous liquid jet. *Phys. Fluids* **29,** 52.

Li, H.-S. (1992) The instability of a liquid jet in a compressible airstream. Ph.D. thesis, Department of Mech. & Aero. Engrn, UCLA, Los Angeles, CA.

McNallen, M. J. and King, T. B. (1982) Fluid dynamics of vertical submerged gas jets in liquid metal processing systems. *Metall. Trans. B* **13B,** 165.

Monkewitz, P. A. (1990) The role of absolute and convective instability in predicting the behavior of fluid systems. *Eur. J. Mech., B/Fluids* **9,** 395.

Ozawa, Y. and Mori, K. (1983) Behavior of gas jets injected into a two-dimensional liquid metal bath. *Trans. I.S.I.J.* **23,** 759.

Ozawa, Y. and Mori, K. (1983) Characteristics of jetting observed in gas injection into liquid. *Trans. I.S.I.J.* **23,** 764.

Payne, G. J. and Price, R. G. (1975) The transition from jetting to bubbling at a submerged orifice. *Trans. Instn Chem. Engrs* **53,** 209.

Prince, M. J. and Blanch, H. W. (1990) Bubble coalescence and break-up in air sparged bubble columns. *AIChE J.* **36,** 1485.

Rayleigh, L. (1879) On the instability of jets. *Proc. London Math. Soc.* **10,** 4.

Sturrock, P. A. (1958) Kinematics of growing waves. *Phys. Rev.* **112,** 1488.

Taylor, G. I. (1945) Generation of ripples by wind blowing over a viscous fluid. In *The Scientific Papers of G. I. Taylor*. Cambridge University Press, London, 1963.

Zhao, F. and Irons, G. (1990) The break-up of bubbles into jets. *Metall. Trans. B* **21B,** 997.

Zhou, Z. W. and Lin, S. P. (1992) Absolute and convective instability of a compressible jet. *Phys. Fluids* **A4,** 277.